Molecular BioSystems

Accepted Manuscript

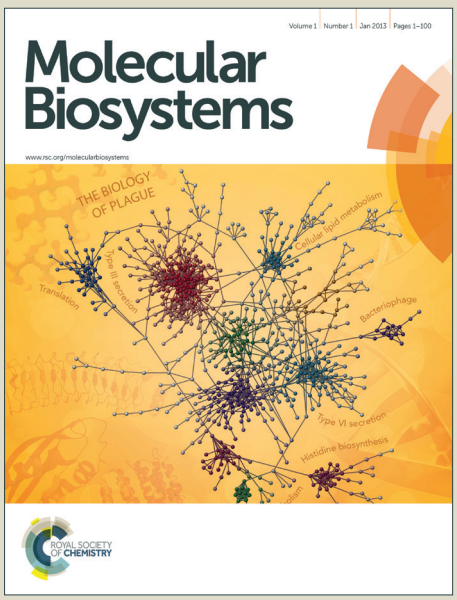

ROYAL SOCIETY OF CHEMISTRY

www.rsc.org/molecularbiosystems

Proteomic analysis of the cytotoxic effects induced by the organogold(III) complex Aubipy$_c$ in cisplatin-resistant A2780 ovarian cancer cells. Further evidence for the glycolytic pathway implication.[§]

Tania Gamberi,[a]* Francesca Magherini,[a] Tania Fiaschi,[a] Ida Landini,[c] Lara Massai,[b] Elisa Valocchia,[a] Laura Bianchi,[e] Luca Bini,[e] Chiara Gabbiani,[d] Stefania Nobili,[c] Enrico Mini,[c] Luigi Messori[b]* and Alessandra Modesti[a]

[a] *Department of Biomedical, Experimental and Clinical Sciences "Mario Serio", University of Florence, Florence, Italy*
[b] *Department of Chemistry, University of Florence, Italy*
[c] *Department of Health Sciences, Section of Clinical Pharmacology and Oncology, University of Florence, Italy*
[d] *Department of Chemistry and Industrial Chemistry, University of Pisa, Italy*
[e] *Functional Proteomic Section, Department of Life Sciences, University of Siena, Italy*

*__Corresponding authors__
Dr. Tania Gamberi, Department of Biomedical, Experimental and Clinical Sciences "Mario Serio", University of Florence, Viale Morgagni 50, 50134 Florence, Italy.
e-mail: tania.gamberi@unifi.it
phone +390552751234
fax +390554598905

Prof. Luigi Messori, Department of Chemistry "Ugo Schiff", University of Florence,
Via della Lastruccia, 3-13, 50019 Sesto Fiorentino, Florence, Italy.
e-mail:luigi.messori@unifi.it
phone +390554573388
fax +390554573385

Textual Abstract

The cytotoxic mechanisms of organogold(III) complex Aubipy$_c$ in cisplatin-resistant A2780 ovarian cancer cells were investigated by 2D-MS. The functional analysis of proteomic data revealed an impairment of glucose metabolism.

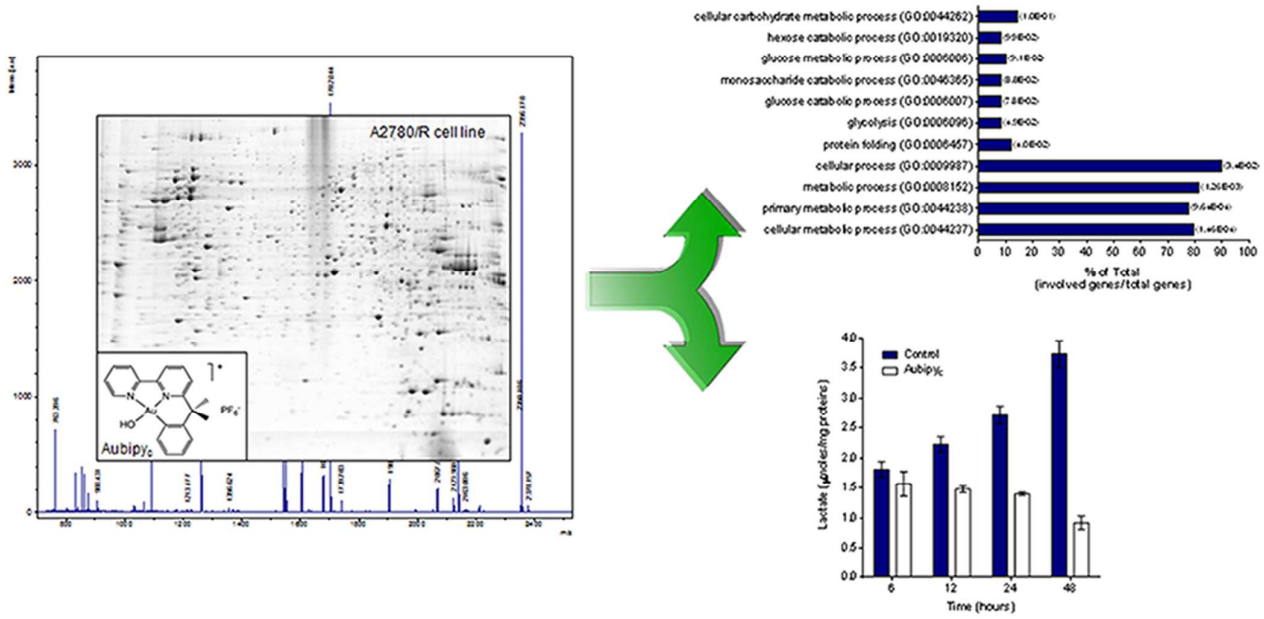

Abstract

The cellular alterations produced in cisplatin-resistant A2780 ovarian cancer cells (A2780/R) upon treatment with the cytotoxic organogold(III) complex Aubipy$_c$ were investigated in depth through a classical proteomic approach. We observed that A2780/R cells exposure to a cytotoxic concentration of Aubipy$_c$ for 24 hours results into a conspicuous number of alterations in protein level that were carefully examined. Notably, we observed that several affected proteins belong to the glucose metabolism system further supporting the idea that the cytotoxic effects of Aubipy$_c$ in A2780/R cells are mostly mediated by an impairment of glucose metabolism in excellent agreement with previous observations on the parent cisplatin-sensitive cell line.

Introduction

Ovarian cancer is the leading cause of gynecological cancers. The most common form is epithelial ovarian cancer that is characterized by few nonspecific early symptoms and by a typical presentation only at an advanced stage, thus, explaining the poor survival statistics.[1,2]

Platinum compounds, given as a combination of cisplatin and carboplatin, are the most active chemotherapeutic agents for this disease and represent the standard treatment for nearly all women diagnosed with ovarian cancer. Although most patients initially respond to this treatment, few are cured.[3,4] Resistance to chemotherapy is the major cause of treatment failure; resistance to cisplatin occurs in roughly one-third of women during primary treatment. Platinum-resistant disease is usually treated with non-platinum based chemotherapy regimens with a modest effect on outcome.[3,4] Several mechanisms have been implicated in causing chemoresistance to cisplatin, such as an increased repair of cisplatin–DNA adducts; changes in the expression of cytochrome P450 genes; alterations in the relevant apoptosis and survival pathways. Despite multiple pathways associated with drug resistance have been pinpointed by many previous studies, the underlying complex mechanisms of cisplatin resistance are far from being fully understood.[5]

Because of widespread cisplatin resistance, there is an increasing interest in the development of non-cisplatin-type metal complexes as anticancer drug candidates for ovarian cancer. In recent years, organometallic compounds with a coordinated gold atom in the oxidation states +1 and +3 were in focus of several studies demonstrating a strong cytotoxicity in several cancer cell lines.[6-8] So far, the most important classes of cytotoxic gold compounds under study as prospective anticancer drug candidates have been gold(III) porphyrins,[9,10] gold(III) dithiocarbamates,[11,12] cyclometalated gold(III) complexes,[13] dinucleargold(III) complexes,[14,15] goldcarbenes[16,17] and 2,3,4,6-tetra-o-acetyl-l-thio-β-D-glucopyranosato-S-(triethyl-phosphine) gold(I) (manufactured as auranofin).[18]

Gold(III) complexes display the same electronic configuration (d^8) and somewhat similar structural and reactivity features to platinum(II) complexes;[19] yet, their mechanisms of action appear to be profoundly different. Previous studies revealed that DNA is not indeed the main target for most gold-based cytotoxic agents – at variance with platinum drugs.[20] Conversely, there is some solid evidence that cytotoxic gold(III) compounds may trigger cell death by targeting various cellular systems: by affecting mitochondria and redox balance,[21,22] modulating cell cycle control,[23] proteolysis,[24] and signal transduction.[25] In particular, there are suggestions that gold-based drugs mainly act through modification of selected proteins with consequent loss of function. Thus, the selective ‘‘protein metalation’’ could be the key feature in the mechanism of action of anticancer gold drugs.[26] An excellent example is offered by the case of the seleno-enzyme thioredoxin

reductase, a putative and now partially validated target for several cytotoxic gold compounds.[27] Irreversible inhibition of human glutathione reductase by phosphine–metal complexes, which results in a unique S–Au(I)–S coordination, has also been found.[28]

Aubipy$_c$ is a promising gold(III) compound that was extensively characterised, both chemically and biologically, through a few recent studies.[29,30] It consists of a square planar gold(III) centre receiving three donor atoms –i.e. C,N,N- from the terdentatebypyridyl ligand while the fourth coordination position is occupied by a hydroxide group (Fig. 1); the latter is the preferential site for ligand replacement reactions and for protein binding. Aubipy$_c$ is acceptably stable under physiological conditions, even in the presence of reducing agents. Previous studies revealed that Aubipy$_c$ exhibits an appreciable cytotoxicity toward the human ovarian cancer cell line A2780, being able to induce apoptotic cell death and to overcome resistance to platinum.[29] However, details of the molecular mechanism leading to mitochondrial damage and consequent induction of apoptosis remain unexplored and warrant further studies.

Recently, to better understand the mechanism of action of Aubipy$_c$, we analysed proteomic alterations induced by this gold compound in a human ovarian cancer cisplatin-sensitive cell line (A2780/S).[31] We found that most of the affected proteins were involved in glucose metabolism, stress response and cell redox homeostasis. Remarkably, the bioinformatics and functional analysis of the proteomic data pointed out quite clearly that Aubipy$_c$ treatment lead to a down-regulation of the glycolytic pathway. To further confirm these mechanistic results, in the present study, we performed a parallel proteomic analysis on the cellular effects of Aubipy$_c$ on cisplatin-resistant A2780 cancer cells (A2780/R). It emerged that gold treatment induced proteomic modifications similar to that achieved in A2780/S cells. Indeed, Aubipy$_c$ mainly acted by affecting glycolytic pathway. This work therefore strengthens the role of glycolysis in Aubipy$_c$ cytotoxic mechanism of action.

Results

Cytotoxic effects of Aubipy$_c$

The antiproliferative properties of Aubipy$_c$ were measured in A2780/R (cisplatin-resistant) cell line, and compared with that of cisplatin, as reported in the Experimental section. The IC_{50} values, observed after exposure to both Aubipy$_c$ and cisplatin, are reported in Table 1. After 24 h of exposure to Aubipy$_c$, IC_{50} value was 28.87 μM whereas that of cisplatin was higher (i.e. > 100 μM). A substantial cytotoxic activity was observed after 72 h of exposure to Aubipy$_c$. IC_{50} value of Aubipy$_c$ (9.90 μM) was lower than IC_{50} of cisplatin (i.e. 24.89 μM). These data were in line with the antiproliferative properties emerged in the Oncotest where Aubipy$_c$ turned out to be one of the

most active gold(III) complexes on the A2780 line and it was found to be able to overcome resistance to cisplatin.[32]

Proteomic analysis

To characterize in detail the cytotoxic mechanisms of $Aubipy_c$, the protein modifications induced by gold treatment in cisplatin-resistant A2780 ovarian cancer cell line (A2780/R) were analysed by two-dimensional electrophoresis (2-DE) approach. A2780/R cells were treated for 24 h with $Aubipy_c$ at a concentration of 10 μM corresponding to its 72-h-exposure IC_{50} in order to reduce the cell death. Indeed, a time course at 24, 48 and 72 h drug exposures with 10 μM of $Aubipy_c$, by using trypan blue vital dye exclusion assay, was performed. After 24 h of exposure, the percentage of cell growth inhibition was 6.7% and the viability of the adherent cells was 95.7%. As expected, cell growth inhibition further increased at 48 h and 72 h of drug exposure reaching 37.2 and 50.7%, respectively, and the viability of the adherent cells decreased to 90.2 and 87.3%, respectively (Table S1) (ESI‡).

After $Aubipy_c$ treatment (10 μM, for 24 h), cellular protein extracts were prepared and separated by 2-D gel electrophoresis as reported in Experimental section, and the resulting 2-DE gels were stained using a modified Neuhoff's colloidal Coomassie Blue G-250 stain ("blue silver").[33] To obtain statistically significant results, we performed three independent experiments for both $Aubipy_c$-treated and -untreated cells. Moreover, in order to minimize gel-to-gel variation, 2-DE was performed twice for each biological replicate and, six gels were indeed analysed for both $Aubipy_c$-treated and control cells. In Fig. 2, representative 2-DE gels of control (Fig. 2A) and $Aubipy_c$-treated A2780/R cells (Fig. 2B) are shown. The 2-DE gel images were analysed by Progenesis SameSpots software v4.0 (Nonlinear Dynamics, UK) using default parameters. After automatic spot detection, an average of about 1,800 protein spots was found in each gel. The computational 2-DE gel image analysis pointed out 70 differentially abundant protein spots (ANOVA p-value$\leq$0.05). The False Discovery Rate (FDR) correction method was then applied in order to reduce the number of false positive.[34] Moreover, we evaluated the reliability of our statistical analysis (power analysis).[35] In our experiments, we achieved a target value of 87% confirming that the number of sample replicates used was appropriate. Therefore, we considered as statistically differentially abundant the protein spots with a corrected p-value (FDR) $\leq$0.05 and a power level $\geq$0.8. Then, we found 57 statistically differentially abundant protein spots. Among them, 35 were more abundant whereas 22 were less abundant in $Aubipy_c$-treated cells with respect to control cells. Such protein spots are highlighted with circles and numbers in the representative gels shown in Fig. 2. These spots were successfully identified by MALDI TOF mass spectrometry. Obtained results are shown in Table 2, where Mascot search results, i.e. score, number of matched peptides and sequence

coverage, are listed. It is noteworthy that more than one protein spot was found to correspond to the same protein, consistently with the presence of different post-translationally modified forms of the same protein (Table 2). For example, we identified three spots as GAPDH: spot 48 with the higher molecular mass, 41 kDa, and spots 52 and 54 with lower molecular masses, 35 kDa and 36 kDa, respectively. Co- and post-translational modifications are actually well known to generate different isoforms of the same protein. According to affected theoretical isoelectric point (pI) and molecular mass (Mr) values, such isoforms are usually resolved in different spots. Several 2-DE studies report a number of different GAPDH isoforms resolved, and identified, in different spots on 2-D gels.[36,37] In some instances, the same protein was identified in spots that displayed a strong discrepancy between the observed position on 2-DE gels and the normal Mr, with a shift toward lower mass (e.g. spots 11, 21, 35, 50) suggesting the presence of protein fragments (Table 2, Fig. 2). Moreover, two differentially abundant protein spots (1 and 11) were found to be coded by the same gene HSPA4L. In particular, in Aubipy$_c$-treated cells, we observed the decrease of the full-length protein amount (spot 1) with a concomitant increase of protein spot with lower Mr (spot 11), suggesting the presence of protein degradation. Thus, the number of unique identified proteins was 48.

All the identified proteins were clustered into functional categories based on the Gene Ontology (GO) terms related to their main biological functions as reported in UniprotKB database (http://www.uniprot.org/). Proteins were clustered in 10 classes and, in Fig. 3, we reported the percentage of identified proteins annotated in each functional category. Most of the proteins was related to the category of metabolism (35.1%), protein synthesis (19.3%) and stress response and chaperones (14%). The remaining identified proteins are shared out among cell cycle and apoptosis (7%), signal transduction (7%), cytoskeleton and cell structure (5.3%), transport (5.3%), cell redox homeostasis (3.5%), DNA replication and repair (1.75%), and unknown (1.75%).

Functional GO terms and pathway enrichment analysis

To gain an overall picture of the cellular changes determined by Aubipy$_c$ treatment, we sought to see whether any GO biological category was statistically over-represented among the differentially abundant proteins we identified. To this aim, we uploaded the list of the identified proteins in the web-accessible program DAVID (Database Annotation Visualization and Integrated Discovery version 6.7; http://david.abcc.ncifcrf.gov/home.jsp).[38,39] A Fisher's enrichment statistical analysis was carried out by comparing the frequencies of the annotation terms in each protein subset with that of the whole list. Figure 4 displays the obtained GO Biological Process (BP) terms statistically over-represented (p-value≤0.1 after Benjamini correction). Detailed composition and statistical parameters were reported in Table S2 (ESI[‡]). Most of the top score biological processes, enriched by the 57 identified proteins, included ontologies involved in metabolism and energy production

such as 'cellular metabolic process' (GO:0044237), 'primary metabolic process' (GO:0044238), 'metabolic process' (GO:0008152) and 'glycolysis' (GO:0006096). Several glycolytic enzymes such as glyceraldehyde-3-phosphate dehydrogenase (GAPDH), alpha enolase (ENO1), fructose-bisphosphatealdolase C (ALDOC) were included in these categories. We also found mitochondrial proteins involved in energy production such as ATP synthase subunit beta, and dihydrolipoyl dehydrogenase DLD (Table S2) (ESI[‡]).

In parallel to this GO BP enrichment analysis, we searched for statistically enriched pathways through DAVID software. We found over-represented the 'glycolysis' term with KEGG pathway (*p*-value <0.05 after Benjamini correction) and the 'metabolism of carbohydrates' term with Reactome pathway (*p*-value <0.05 after Benjamini correction). The proteins associated with the term 'glycolysis', are ALDOC, GAPDH, ENO1, LDHB and DLD (Table 3).

Protein validation by 2-D Western blot

Two dimensional electrophoresis followed by Western blot analysis was used to validate some of the changes in protein abundance of the glycolytic enzymes revealed by 2-DE/MS analysis. The validation was performed for GAPDH and ENO1 in A2780/R cells treated for 24 h with 10 μM Aubipy$_c$. Representative 2-D immunoblots were shown in Fig. 5A. For each tested protein, the optical density of specific immunoreactive spot was detected and their values were statistically analysed by two-tailed non-paired Student's-*t*-test. The resulting mean values ± SD, of three independent experiments, were reported in the histograms in Fig. 5B and 5C. As expected, we found that A2780/R treated cells displayed changes for these glycolytic enzymes similar to that observed in 2-DE gels. In particular, we found two immunoreactive GAPDH spots, corresponding to 2-DE spots 52 and 54, with a three and two-fold abundance increase, respectively, and another immunoreactive spot, the 2-DE spot 48, with a three-fold decrease. As regards ENO1, we detected two immunoreactive spots, spot 31 and spot 32, that showed a two-fold increased amount.

Metabolic investigations

Proteomic and bioinformatic results suggested a possible cytotoxic effect of Aubipy$_c$, directly or indirectly, on glycolysis pathway. To strengthen these data, we evaluated the ability of Aubipy$_c$-treated cells to consume glucose and to generate lactate. Glucose and lactate concentrations were measured in one millilitre of medium supernatant harvested after 6, 12, 24, 48 h the addition of 10 μM Aubipy$_c$. Experiments were performed in triplicate. The resulting mean values ± SD were reported in the histograms in Fig. 6. The glucose assay pointed out that up to 24 hours glucose amount in the medium was similar in treated and untreated cells (Fig. 6A). After 48, the glucose level was statistically higher in Aubipy$_c$-treated cells (*p*-value<0.05 by two-tailed non-paired Student's-*t*-test). Indeed, in treated cells, we measured a glucose level of about 2 times higher than

in control cells suggesting an impairment in glucose utilization. Concerning lactate production, we found that after 6 h of treatment the lactate level was similar in treated and untreated cells (Fig. 6B). The exposure of A2780/R cells to gold compound elicited a clear decrease in their lactate secretion after 12 hours. The lactate amount was 1.5 times statistically lower in Aubipy$_c$-treated cells (p-value<0.05). The lower lactate production in treated cells became more evident after 24 and 48 hours. Indeed, we assessed a lactate level of about two and four times lower, respectively, then in untreated cells. In order to investigate a possible functional relationship between these results and the decrease in LDHB abundance pointed out by 2D-MS analysis, we assessed the amount of this enzyme by western blot analysis. The western blot was performed in cells treated with 10 μM Aubipy$_c$ for 6, 12, 24, 48 h. Representative immunoblots were shown in Fig. 6C. For each time point, the optical density of specific immunoreactive band was detected and its value was statistically analysed by two-tailed non-paired Student's-t-test. The resulting mean values ± SD, of three independent experiments, were reported in the histogram in Fig. 6C. We found, in Aubipy$_c$-treated cells, a decrease in LDHB amount after 12 h (about 1.8 fold), thus at the same time point in which the gold compound induced a decrease in lactate secretion. The LDHB decrease was more evident after 24 h (about 2 fold) and 48 h of treatment (about 3 fold).

Discussion

Aubipy$_c$ is a promising gold(III) compound which manifests an appreciable cytotoxicity toward the cell line A2780. Our previous proteomic study reporting the effects of Aubipy$_c$ on A2780 cisplatin-sensitive cells pointed out that gold treatment affected, directly or indirectly, several glycolytic enzymes.[31] In the present study, we extended the investigation to the cisplatin resistant subline A2780/R obtained from the parental cisplatin sensitive cell line A2780. We aimed to highlight the Aubipy$_c$ mechanism of action and to evaluate if this gold compound were able to affect proteins or biological processes/functions relevant in the acquisition of platinum-based drug resistance. Thus, we carried out a comparative proteomic study using 2-DE coupled with mass spectrometry. The results pointed out 57 differentially abundant proteins following Aubipy$_c$ treatment. Among them, 35 proteins resulted more abundant and 22 less abundant. These proteins play specific roles in a variety of biological processes. Most of them belong to functional three functional classes: metabolism, protein synthesis, and stress response and chaperones. In order to understand the biological meaning behind the list of 57 identified proteins, we processed them using the web-accessible program DAVID. This bioinformatics resource provides information about the GO terms enriched by a dataset of proteins or genes. The GO BP term protein folding resulted statistically enriched; it includes several members of the heat shock family, such as heat shock 70kDa protein

4L, stress-70 protein mitochondrial and two forms of T-complex protein 1 subunit beta (CCT2). Heat shock proteins (HSPs) are over-expressed in a wide variety of human cancer cells[40] and some of them, such as Hsp27 and Hsp70, are involved in the prognosis of specific cancer types.[41] Furthermore, several studies reported an increase of HSPs expression upon exposure to anticancer agents. These chaperones may participate in the stress response to drug-induced damage.[42] In line with these data, Aubipy$_c$ led to an increase of the amount of two forms of T-complex protein 1, subunit beta (CCT2). The TCP-1 chaperonin family known as 'eukaryotic cytosolic chaperonin containing TCP-1 (CCT) has a critical function in the folding of many proteins, including the cytoskeletal components actin and tubulin.[43] T-complex protein 1 subunits were already found to be involved in the process of chemoresistance by Castagna *et al.*[44] Conversely, the level of the other identified HSPs (HSPAL4, HSPA9, FKBP4, AHSA1) decreased upon gold treatment. Concerning HSPAL4, we observed the decrease of the full- length protein amount with a concomitant increase of a protein form with lower Mr, suggesting the presence of protein degradation. HSPA9 is over-expressed in human malignancies. Yang et *al.* demonstrated that elevated levels of HSPA9 increase cancer cell resistance to cisplatin-induced cytotoxicity.[45] FKBP4 belongs to a subclass of FK506-binding proteins.[46] Several studies have proposed FKBP4 as a biomarker for tumorigenesis that provides chemoresistance through several different signaling pathways.[47] Based on the observed increased expression of these HSPs in cancer cells, its proposed role in metastasis and its anti-apoptotic properties, we hypothesized that Aubipy$_c$ treatment could induce cell death and overcome resistance to cisplatin, at least in part, through an impairment of protein folding machinery.

We also observed an enrichment of GO BP terms involved in metabolism and energy production, such as cellular metabolic process, glucose metabolic process, and glycolysis. Most of the proteins involved in this enrichment are glycolytic enzymes, such as ENO1, GAPDH, ALDOC, and LDHB but also mitochondrial enzymes active in cellular respiration, such as dihydrolipoyl dehydrogenase (DLD) and ATP synthase subunit beta (ATP5B). In line with these data, the list of differentially abundant proteins also statistically enriched the GO pathway terms glycolysis and metabolism of carbohydrates. Worthy of note, some glycolytic enzymes involved in this functional analysis increased in abundance (ENO1 and two forms of GAPDH) while others (ALDOC, LDHB and a form of GAPDH) decreased after gold treatment. This trend was validated, regards to GAPDH and ENO1, by 2-D Western blot analysis. Multiple forms of GAPDH were detected in cancer cell lines and normal tissue by two-dimensional electrophoresis and Western blot analysis. These forms, that differed by pI and Mr, may play diverse roles in normal tissue and in cancer.[48] Genes of glucose metabolism have been reported to be ubiquitously over-expressed in cancer cells[49] and energy production is abnormally dependent on aerobic glycolysis.[50] The glycolytic shift in tumor cells

compensates for mitochondrial dysfunction and provides resistance to apoptosis. Moreover, these metabolic alterations are responsible for chemoresistance in cancer therapy. Glyceraldehyde-3-phosphate dehydrogenase and alpha enolase seem to be relevant in the acquisition of drug resistance in cancer cell lines, due to their transcriptional regulation activity more than to their function in glycolysis.[51]

It is noteworthy that some of these glycolytic enzymes pointed out by 2D-MS analysis, such as ENO1 and GAPDH, were also found to be affected by Aubipy$_c$ in A2780/S cell line[31]. Others, such as ALDOC and LDHB, were identified only in this study on A2780/R. These differences could be related to biological processes/functions that are modulated in sensitive or resistant cell lines and relevant in the acquisition of drug resistance. Indeed, in previous studies, these two enzymes were found to be over-expressed in cisplatin-resistant A2780 cell line.[52,53]

In order to understand whether changes in abundance of these glycolytic enzymes could affect glycolysis we assessed glucose consumption and lactate production after gold treatment. The obtained results pointed out that Aubipy$_c$ led to a lower lactate production following by a reduction in glucose consumption. These findings were supported by the western blot against LDHB. We found a decrease of this enzyme after 12 h of Aubipy$_c$ treatment, thus at the same time point in which the gold compound produced a clear decrease in lactate secretion. It is known that LDHA kinetically favors the conversion of pyruvate to lactate in aerobic glycolysis and is therefore important for tumorigenesis.[54] LDHB could also mediate the same reaction, although it is more sensitive to substrate (pyruvate) inhibition and hence is thought to favour the conversion of lactate to pyruvate.[54] Despite this, the association of LDHB with cancer is complex. LDHB gene is silenced in several cancer types but is overexpressed or amplified in others, for example in human lung adenocarcinoma with KRAS mutation and in testicular germ cell tumors.[55] In addition, LDHB rather than LDHA appears to be necessary for triple-negative breast cancer.[56] Hence, the roles of LDHA and LDHB in aerobic glycolysis or in mitochondrial respiration in specific types of human cancers remain to be fully established. We can conclude that, at least as regards A2780/R cell line, there is a functional link between the decrease in lactate production and LDHB down-regulation.

Hence, our functional proteomic analysis highlighted a potential negative effect of Aubipy$_c$ on glucose metabolism that causes glycolysis slowdown. This slowdown of glycolytic pathway in A2780/R cells raised the question of whether glycolytic enzymes could be affected directly or indirectly by Aubipy$_c$ treatment. Go Ym *et al.* demonstrated, by proteomic analysis, that the gold(I) compound Auranofin (ARF) oxidized peptidylCys associated with proteins of glycolysis and gluconeogenesis in human colon carcinoma HT29 cells.[57] Moreover, to verify ARF-inhibition of glycolysis, they examined HT29 cells for pyruvate kinase (PK) enzyme activity and lactate amount.

The result showed that both PK activity and lactate levels were significantly decreased by ARF treatment confirming the previously study on ARF-dependent inhibition of glycolysis in human neutrophils.[57] Given that ARF and Aubipy$_c$ are both Au-based drugs, we suppose that Aubipy$_c$ could also be able to oxidize the Cys residues of proteins involved in the glycolytic enzymatic pathways. Additional studies are needed to demonstrate this hypothesis.

Experimental

Materials

RPMI 1640 cell culture medium, fetal calf serum (FCS), and phosphate-buffered saline were obtained from Celbio (Milan, Italy); sulforhodamine B (SRB) and cisplatin were obtained from Sigma (Milan, Italy). General chemicals were purchased from Sigma Aldrich (Italy), unless otherwise indicated.

Cell lines and culture conditions

The human ovarian carcinoma cell line resistant to cisplatin (A2780/R) was used for cytotoxicity and proteomic studies. Cells were maintained in RPMI1640 medium supplemented with 10% of FCS and antibiotics at 37°C in a 5% CO2 atmosphere and sub-cultured twice weekly.

Cell growth inhibition studies

The cytotoxic activity of Aubipy$_c$ was evaluated against the A2780/R cell line according to the method described by Skehan *et al.*[58] Aubipy$_c$ was diluted in DMSO as stock solution (10 mM). Exponentially growing cells were seeded in 96-well microplates at the density of $5x10^3$ for 24 h prior to the addition of Aubipy$_c$. After 24 h, the medium was removed and replaced with fresh medium containing concentrations of Aubipy$_c$ ranging from 0.003 to 100 μM. Two different times of exposure to Aubipy$_c$, 24 and 72 h, were used. For comparison purposes, the cytotoxicity of cisplatin was evaluated in the same experimental conditions. Then the cells were fixed with trichloroacetic acid and then stained with sulforhodamine B (SRB) solution, rinsed with 0.1% acetic acid and air-dried. At the end of the staining period, SRB was dissolved in 10 mM Tris–HCl solution (pH 10.5). Optical density was read in a microplate reader interfaced with the software Microplate Manager/PV version 4.0 (Bio-Rad Laboratories, Milan, Italy) at 540 nm. The IC_{50} drug concentration resulting in a 50% reduction in the net protein content (as measured by SRB staining) in drug-treated cells as compared with untreated control cells was determined.

Trypan blue vital dye exclusion assay

A trypan blue vital dye exclusion assay was carried out to evaluate the viability of cells to be used in the proteomic studies. Briefly, we performed a time course at 24, 48 and 72 h drug exposures with 10 μM of Aubipy$_c$ (equal to 72-h-exposure IC50 value). Following exposures, 200 μL of

trypsinized and re-suspended cells were mixed with 200 µL of 0.4% solution of trypan blue dye (Sigma-Aldrich) for 5 min. Numbers of total cells, live cells and dead cells, were immediately counted using a Neubauer micro-chamber (Brand GmbH, Wertheim, Germany) with a light microscope. All counts were done in duplicates of each sample. The reported data represent the mean of three independent experiments.

Two-dimensional gel electrophoresis

A2780/R cells were seeded in tissue-culture plates at 5×10^4 cells/mL (total volume 30 mL) and incubated overnight, then exposed to concentration of the $Aubipy_c$ equal to 72-h-exposure IC_{50} values for 24 h (10 µM) or to an equal concentration of DMSO. After that, the cells were washed with phosphate-buffered saline and then scraped in RIPA buffer (50 mM Tris-HCl pH 7.0, 1% (v/v) NP-40, 150 mMNaCl, 2 mM ethylene glycol bis(2-aminoethyl ether)tetra-acetic acid, 100 mM NaF) containing a human protease inhibitor cocktail (Sigma). The cells were sonicated (15 s) and protein extracts were clarified by centrifugation at 8,000*g*, 4°C for 15 min. Proteins were precipitated following a chloroform/methanol protocol[59] and the protein pellets were resolved in a buffer containing 8 M urea, 4% (w/v) 3-cholamidopropyl dimethylammonium-1- propane sulfonate (CHAPS), 65 mM dithioerythritol (DTE). Protein concentration was determined by the standard Bradford method (Bio-Rad). Isoelectric focusing (IEF) was carried out on nonlinear wide-range immobilized pH gradient (pH 3–10; 18-cm-long IPG strip; Bio-Rad) and achieved using an EttanIPGphor™ system (GE Healthcare). Protein sample (700 µg) was cup-loaded near the anode in the EttanIPGphor Cup Loadind Manifold™ (GE Healthcare) after the rehydration of the IPG strips with 350 µl of rehydration solution (8 M urea,2% (w/v) CHAPS, 0.5% (w/v) DTE) supplemented with 0.5% (v/v) carrier ampholyte (Bio-Rad) and a trace of bromophenol blue, overnight at room temperature. The strips were focused at 16°C according to the following electrical conditions: 200 V for 1 h, 300 V for 1 h, from 300 to 3,500 V in 30 min, 3,500 V for 4h, 5,000 for 2h, from 5,000 to 8,000 V in 30 min, and 8,000 V until a total of 100,000 V/ h was reached, with a limiting current of 50 µA/strip. After focusing, strips were equilibrated in 6 M urea, 2% (w/v) SDS, 2% (w/v) DTE, 30% (v/v) glycerol and 0.05 M Tris-HCL pH 6.8 for 10 min and, subsequently, for 10 min in the same urea/SDS/Tris-HCl buffer solution where DTE was substituted with 2.5% (w/v) iodoacetamide (IA). The equilibrated strips were placed on top of 9–16% polyacrylamide linear gradient gels (18 cm × 20 cm × 1.5 mm) and embedded in 0.5% (w/v) heated low-melting agarose in SDS electrophoresis running buffer (25 mMTris, 192 mM glycine, 0.1% (w/v) SDS, pH 8.3). The methylenebisacrilamide was the cross-linker used in the 9-16% gradient. SDS-PAGE was performed in a PROTEAN II xi cell gel electrophoresis unit (Bio-Rad) at

10°C and at 40mA/gel constant current, until the dye front reached the bottom of the gel, according to Hochstrasser *et al*.[60] Gels were stained with colloidal Coomassie blue silver.[33]

Image analysis and statistics

Three independent Aubipy$_c$ treatment were performed (biological replicates) and for each sample two 2-DE were carried out (technical replicates), so that in total 12 gels were analysed (6 gels for both A2780/R Aubipy$_c$-treated and control cells). Colloidal Coomassie blue silver-stained gels were scanned using the Epson expression 1680 PRO scanner. The gel images were saved with a resolution of 300 dpi and as 16-bit TIFF format. Image analysis was carried out using the Progenesis SameSpots software v4.0 (Nonlinear Dynamics, UK) which allows spot detection, background subtraction and protein spot volume quantification. The gel image showing the highest number of spots and the best protein pattern was chosen as the reference image and its spots were then matched across all gels. This reference image was used to quantify and normalize the spot volumes. The spot volumes were normalized in each gel as relative volume (volume percentage), by dividing the raw quantity of each spot by the total quantity of all the spots included in the reference gel. Statistical analysis was performed using default parameters of the Progenesis SameSpots Stat module. The $\log_{10}$-normalized spot volume was used for the analysis as the log transformation improves normality.[61] The univariate data analysis was performed as one-way ANOVA on each spot individually. Then, a multivariate statistics was applied on all the ANOVA *p*-values by the False Discovery Rate (FDR) correction method.[34] Moreover, we performed a power analysis to assess the number of sample replicates that need to be analysed in order to confidently discover differentially abundant proteins. The accepted power threshold is ≥0.8.[62] We considered statistically differentially abundant spots those having a corrected *p*-value (FDR) ≤0.05 and a power ≥0.8. These spots were subjected to mass spectrometry analysis.

Mass spectrometry analysis

Electrophoretic spots were manually excised, destained, and acetonitrile dehydrated. A trypsin solution (0.25mg/ml) in 50 mM ammonium bicarbonate was added for in-gel protein digestion by overnight incubation at 37°C. Solutions containing digested peptides were recovered and 20 µl of 1% TFA 50% ACN were added to each spot and sonicated for 10 minutes to maximize peptide recovery. At the end, for each spot all recovered peptide solutions were combined and concentrated. From each protein digest 0.75 µl were spotted onto the MALDI target and allowed to air dry at room temperature. Then, 0.75 µl of matrix solution (saturated solution of α-cyano-4-hydroxycinnamic acid in 50% (v/v) acetonitrile and 0.5% (v/v) TFA) was applied to the sample and crystallized by air drying at room temperature for 5 min. Protein identification was carried out by peptide mass fingerprinting (PMF) on an Ultraflex III MALDI-TOF/TOF mass spectrometer

(Bruker Daltonics) equipped with a 200 Hz smartbeam™ I laser. MS analysis was performed in the positive reflector mode according to defined parameters, as follows: 80 ns of delay; ion source 1: 25 kV; ion source 2: 21.75 kV; lens voltage: 9.50 kV; reflector voltage: 26.30 kV; and reflector 2 voltage: 14.00 kV. The applied laser wavelength and frequency were 353 nm and 100 Hz, respectively, and the percentage was set to 46%. Final mass spectra were produced by averaging 1500 laser shots targeting five different positions within the spot. Spectra were acquired automatically and the Flex Analysis software version 3.0 (Bruker) was used for their analysis and for the assignment of the peaks. The applied software generated a list of peaks up to 200, using a signal-to-noise ratio of 3 as threshold for peak acceptance. Recorded spectra were calibrated using, as internal standard, peptides arising from trypsin auto-proteolysis. The mass lists were filtered for contaminant removal: mass matrix-related ions, trypsin auto-lysis and keratin peaks. Protein identification by Peptide Mass Fingerprint search was established using MASCOT search engine version 2.1 (Matrix Science, London, UK, http://www.matrixscience.com) through the UniProtKB database (http://www.uniprot.org/). Taxonomy was limited to *Homo sapiens*, a mass tolerance of 100 ppm was allowed, and the number of accepted missed cleavage sites was set to one. Alkylation of cysteine by carbamidomethylation was considered a fixed modification, while oxidation of methionine was considered as a possible modification. The criteria used to accept identifications included the extent of sequence coverage, the number of matched peptides, and a probabilistic score at $p<0.05$.

Bioinformatic functional analysis

To identified statistically over-represented (enriched) Gene Ontology (GO) terms among the differentially abundant proteins identified by MS analysis, we used David Bioinformatics Resource (version 6.7) (Database for Annotation, Visualization and Integrated Discovery; http://david.abcc.ncifcrf.gov/)[38,39]. The list of UniProtKB accession numbers of the identified proteins was loaded into the online tool clicking on Functional annotation clustering. After submission of the list, functional classification was performed on the basis of Gene Ontology. Fisher's exact test was used to check for significant over-representation (p-value<0.05) of GO terms in the submitted dataset against the *Homo sapiens* genome. Furthermore Benjamini multiple testing was performed to globally correct the p-value controlling family-wide false discovery rate (p-value ≤0.1).

Two-dimensional Western blot analysis

A2780/R cells were treated for 24 h with $Aubipy_c$ concentration corresponding to its 72-h-exposure IC_{50} dose (10 µM). Protein extracts (150 µg), from control and $Aubipy_c$-treated cells, were separated by 2-DE as previously described and transferred on PVDF membrane (Millipore). The relative

amount of the GAPDH and ENO1 was assessed with appropriate monoclonal antibodies (Santa Cruz Biotechnology). According to datasheets, all antibodies were employed with a 1:1,000 dilution in 2% milk. After incubation with horseradish peroxidase (HRP)–conjugated anti-mouse IgG (1:2,000) (Amersham Biosciences), immunecomplexes were detected with the enhanced chemiluminescence (ECL) detection system (GE Healthcare). The membranes were exposed to autoradiographic films (Hyperfilm MP; (GE Healthcare) for 1–30 minutes. Digitized images of 2-D Western blots were analyzed using the Image Master 2D Platinum 7.0 software (GE Healthcare). The equal loading of samples was ensured by Coomassie brilliant blue staining of PVDF membranes. Statistical analysis, of three independent experiments, was performed by two-tailed non-paired Student's-*t*-test using Graphpad Prism 6. A p-value<0.05 was considered statistically significant.

Glucose and Lactate assay

A2780/R cells were treated for 48 h with $Aubipy_c$ concentration corresponding to its 72-h-exposure IC50 dose (10 µM). One millilitre of medium supernatant was harvested after 6, 12, 24, 48 h the addition of $Aubipy_c$. Glucose concentration was measured using commercially kit based on the glucose oxidase/peroxidase enzymic procedure (K-GLUC from Megazyme). Lactate concentration was assessed using the L-Lactic acid Assay Kit (Megazyme) according to the manufacturer's instructions. Experiments were performed in triplicate. Results were normalized to the cellular protein content. A two-tailed non-paired Student's-*t*-test was performed using Graphpad Prism 6. A p-value<0.05 was considered statistically significant.

LDHB western blot analysis

A2780/R cells were prepared as described in paragraph "Glucose and Lactate assay". Cells were harvested after 6, 12, 24, 48 h the addition of $Aubipy_c$ and lysed in RIPA buffer (50 mM Tris-HCl pH 7.0, 1% (v/v) NP-40, 150 mM NaCl, 2 mM ethylene glycol bis(2-aminoethyl ether)tetra-acetic acid, 100 mM NaF) containing a human protease inhibitor cocktail (Sigma). The cells were sonicated (15 s) and protein extracts were clarified by centrifugation at 8,000g, 4° C for 15 min. Protein samples (15µg) were separated on 4-16% gradient SDS-PAGE precast gels (Bio-rad) and transferred onto a PVDF membrane (Bio-rad). The relative amount of the LDHB was assessed with appropriate polyclonal antibody (AV48210 Sigma, Milan, Italy). According to datasheets, antibody was employed with a 1:1,000 dilution in 2% milk. After incubation with horseradish peroxidase (HRP)–conjugated anti-mouse IgG (1:2,000) (Amersham Biosciences), immune complexes were detected with the enhanced chemiluminescence (ECL) detection system (GE Healthcare). The PVDF membrane was exposed to autoradiographic films (Hyperfilm MP; Amersham Biosciences) for 1–30 minutes. For quantification, blot was subjected to densitometric analysis using Quantity

One Software (Bio-Rad). The intensity of the immuno-stained bands was normalized with the total protein intensities measured by Coomassie brilliant blue R-250 from the same blot. Statistical analysis, of three independent experiments, was performed by two-tailed non-paired Student's-*t*-test using Graphpad Prism 6. A p-value<0.05 was considered statistically significant.

Conclusion

In summary, the data presented herein strongly correlate to the previous study on the human ovarian cancer cisplatin-sensitive cell line (A2780/S). We demonstrated that Aubipy$_c$ induced in these two cell lines similar changes in abundance of proteins. Indeed, the gold compound affected proteins belong to the same functional categories (such as stress response and chaperones, protein synthesis, glucose metabolism). In particular, we found that Aubipy$_c$ affected glycolytic enzymes such as GAPDH and ENO1. However, our proteomic studies also pointed out some differences. In A2780/S we found a decrease in abundance of PKM and PGK1 while in A2780/R we observed a decrease of ALDOC and LDHB. These differences could be related to biological processes/functions that are modulated in sensitive or resistant cell lines and relevant in the acquisition of drug resistance.

The interesting finding of this proteomic study is that it has provided further evidence for the glycolytic implication in the cytotoxic effects of Aubipy$_c$. Based on these data, we can state that a down-regulation of glucose metabolism might explain, at least in part, the biological effects of this gold compound. Yet, it is not possible to establish whether Aubipy$_c$ acts by directly inhibiting the identified glycolytic enzymes or if beyond the slowdown of glycolysis, other molecular mechanisms are operative.

Altogether, our two proteomic studies provide a solid starting point for further study on Aubipy$_c$ mechanism of action. Additional study is actually required to clarify the specific role exert by the other identified proteins (such as HSPs) and their corresponding pathways in cell response to drug-induced damage. Moreover, analyses are needed to demonstrate if Aubipy$_c$ is able to bind directly these proteins or at least some of them.

Acknowledgements

We gratefully acknowledge AIRC (IG-12085) and Ente Cassa di Risparmio di Firenze (MODECRF 130504) for generous financial support. The authors wish to thank Maria Agostina Cinellu of the Department of Chemistry and Pharmacy, University of Sassari, for the gift of a sample of Aubipy$_c$.

Notes

[†]Presented, in part, at the IX Annual Congress of Italian Proteomics Association held in Naples 24th -27th June 2014

[‡]Electronic Supplementary Information (ESI) available: Table S1 and Table S2.

Authors' contributions: TG conceived and designed the experiments, performed 2-DE gel image analysis, wrote manuscript. FM performed 2-DE gels, helped to draft the manuscript. TF contributed in writing the manuscript. EV contributed in performing 2-DE gels. IL performed cell culture experiments. LM contributed in writing the manuscript. L Bianchi performed mass spectrometry and helped to draft the manuscript. L Bini analysed mass spectrometry data and helped to draft the manuscript. CG helped to draft the manuscript. SN analyzed the data of cell culture experiments and helped to draft the manuscript. EM helped to draft the manuscript. LM contributed in writing the manuscript. AM performed the bioinformatics analysis and contributed in writing the manuscript.

All authors read and approved the final manuscript.

References

1 A. Jemal, R. Siegel, J. Q. Xu, and E. Ward, *Ca-A Cancer J. for Clin.*, 2010**, 60**(5), 277-300.

2 B. A. Goff, L. S. Mandel, C. W. Drescher, N. Urban, S. Gough, K. M. Schurman, J. Patras, B. S. Mahony, and M. R. Andersen, *Cancer*, 2007**, 109**(2), 221-227.

3 A. Davis, A. V. Tinker, and M. Friedlander, *Gynecologic Oncology*, 2014**, 133**(3), 624-631.

4 D. Luvero, A. Milani, and J. A. Ledermann, *Therapeutic Advances in Medical Oncology*, 2014**, 6**(5), 229-239.

5 L. Galluzzi, I. Vitale, J. Michels, C. Brenner, G. Szabadkai, A. Harel-Bellan, M. Castedo, and G. Kroemer, *Cell Death & Disease*, 2014**,** DOI: 10.1038/cddis.2013.428.

6 S. Nobili, E. Mini, I. Landini, C. Gabbiani, A. Casini, and L. Messori, *Medicinal Research Reviews*, 2010**, 30**(3), 550-580.

7 S. J. Berners-Price and A. Filipovska, *Metallomics*, 2011**, 3**(9), 863-873.

8 T. T. Zou, C. T. Lum, S. S. Y. Chui, and C. M. Che, *Angewandte Chemie-International Edition*, 2013**, 52**(10), 2930-2933.

9 R. W. Y. Sun, C. K. L. Li, D. L. Ma, J. J. Yan, C. N. Lok, C. H. Leung, N. Y. Zhu, and C. M. Che, *Chemistry-A European Journal*, 2010**, 16**(10), 3097-3113.

10 R. W. Y. Sun and C. M. Che, *Coord. Chem. Rev.*, 2009**, 253**(11-12), 1682-1691.

11 L. Ronconi, L. Giovagnini, C. Marzano, F. Bettio, R. Graziani, G. Pilloni, and D. Fregona, *Inorg. Chem.*, 2005**, 44**(6), 1867-1881.

12 V. Milacic, D. Chen, L. Ronconi, K. R. Landis-Piwowar, D. Fregona, and Q. P. Dou, *Cancer Res.*, 2006**, 66**(21), 10478-10486.

13 M. A. Cinellu, A. Zucca, S. Stoccoro, G. Minghetti, M. Manassero, and M. Sansoni, *Journal of the Chemical Society-Dalton Transactions*, 1996, (22) 4217-4225.

14 C. Gabbiani, A. Casini, L. Messori, A. Guerri, M. A. Cinellu, G. Mlnghetti, M. Corsini, C. Rosani, P. Zanello, and M. Arca, *Inorg. Chem.*, 2008**, 47**(7), 2368-2379.

15 A. Casini, M. A. Cinellu, G. Minghetti, C. Gabbiani, M. Coronnello, E. Mini, and L. Messori, *J. Med. Chem.*, 2006**, 49**(18), 5524-5531.

16 L. Messori, L. Marchetti, L. Massai, F. Scaletti, A. Guerri, I. Landini, S. Nobili, G. Perrone, E. Mini, P. Leoni, M. Pasquali, and C. Gabbiani, *Inorg. Chem.*, 2014**, 53**(5), 2396-2403.

17 L. Oehninger, R. Rubbiani, and I. Ott, *Dalton Transactions*, 2013**, 42**(10), 3269-3284.

18 C. Marzano, V. Gandin, A. Folda, G. Scutari, A. Bindoli, and M. P. Rigobello, *Free Radic.Biol.Med.*, 2007**, 42**(6), 872-881.

19 A. Casini, C. Hartinger, C. Gabbiani, E. Mini, P. J. Dyson, B. K. Keppler, and L. Messori, *J. Inorg. Biochem.*, 2008**, 102**(3), 564-575.

20 C. K. Mirabelli, C. M. Sung, J. P. Zimmerman, D. T. Hill, S. Mong, and S. T. Crooke, *Biochemical Pharmacology*, 1986**, 35**(9), 1427-1433.

21 A. Meyer, C. P. Bagowski, M. Kokoschka, M. Stefanopoulou, H. Alborzinia, S. Can, D. H. Vlecken, W. S. Sheldrick, S. Wolfl, and I. Ott, *Angewandte Chemie-International Edition*, 2012**, 51**(35), 8895-8899.

22 A. Casini and L. Messori, *Curr. Top. Med. Chem.*, 2011**, 11**(21), 2647-2660.

23 S. P. Tu, R. W. Y. Sun, M. C. M. Lin, J. T. Cui, B. Zou, Q. Gu, H. F. Kung, C. M. Che, and B. C. Y. Wong, *Cancer*, 2009**, 115**(19), 4459-4469.

24 M. Serratrice, F. Edafe, F. Mendes, R. Scopelliti, S. M. Zakeeruddin, M. Gratzel, I. Santos, M. A. Cinellu, and A. Casini, *Dalton Transactions*, 2012**, 41**(11), 3287-3293.

25 A. Nakaya, M. Sagawa, A. Muto, H. Uchida, Y. Ikeda, and M. Kizaki, *Leukemia Research*, 2011**, 35**(2), 243-249.

26 L. Messori, F. Scaletti, L. Massai, M. A. Cinellu, C. Gabbiani, A. Vergara, and A. Merlino, *Chemical Communications*, 2013**, 49**(86), 10100-10102.

27 A. Bindoli, M. P. Rigobello, G. Scutari, C. Gabbiani, A. Casini, and L. Messori, *Coord. Chem. Rev.*, 2009**, 253**(11-12), 1692-1707.

28 S. Urig, K. Fritz-Wolf, R. Reau, C. Herold-Mende, K. Toth, E. Davioud-Charvet, and K. Becker, *Angewandte Chemie-International Edition*, 2006**, 45**(12), 1881-1886.

29 G. Marcon, S. Carotti, M. Coronnello, L. Messori, E. Mini, P. Orioli, T. Mazzei, M. A. Cinellu, and G. Minghetti, *J. Med. Chem.*, 2002**, 45**(8), 1672-1677.

30 C. Gabbiani, M. A. Cinellu, L. Maiore, L. Massai, F. Scaletti, and L. Messori, *Inorganica Chimica Acta*, 2012**, 393**, 115-124.

31 T. Gamberi, L. Massai, F. Magherini, I. Landini, T. Fiaschi, F. Scaletti, C. Gabbiani, L. Bianchi, L. Bini, S. Nobili, G. Perrone, E. Mini, L. Messori, and A. Modesti, *J. Proteomics*, 2014**, 103**, 103-120.

32 A. Casini, G. Kelter, C. Gabbiani, M. A. Cinellu, G. Minghetti, D. Fregona, H. H. Fiebig, and L. Messori, *J. Biol. Inorg. Chem.*, 2009**, 14**(7), 1139-1149.

33 G. Candiano, M. Bruschi, L. Musante, L. Santucci, G. M. Ghiggeri, B. Carnemolla, P. Orecchia, L. Zardi, and P. G. Righetti, *Electrophoresis*, 2004**, 25**(9), 1327-1333.

34 Y. Benjamini and Y. Hochberg, *Journal of the Royal Statistical Society Series B-Methodological*, 1995**, 57**(1), 289-300.

35 N. A. Karp and K. S. Lilley, *Proteomics.*, 2007**, 7**, 42-50.

36 M. Di Michele, C. A. Della, L. Cicchillitti, B. P. Del, A. Urbani, C. Ferlini, G. Scambia, M. B. Donati, and D. Rotilio, *Biochim. Biophys. Acta*, 2009**, 1794**(2), 225-236.

37 W. Sun, B. Xing, Y. Sun, X. Du, M. Lu, C. Hao, Z. Lu, W. Mi, S. Wu, H. Wei, X. Gao, Y. Zhu, Y. Jiang, X. Qian, and F. He, *Mol.Cell Proteomics.*, 2007**, 6**(10), 1798-1808.

38 D. W. Huang, B. T. Sherman, and R. A. Lempicki, *Nature Protocols*, 2009**, 4**(1), 44-57.

39 D. W. Huang, B. T. Sherman, and R. A. Lempicki, *Nucleic Acids Research*, 2009**, 37**(1), 1-13.

40 Y. J. Hwang, S. P. Lee, S. Y. Kim, Y. H. Choi, M. J. Kim, C. H. Lee, J. Y. Lee, and D. Y. Kim, *Yonsei Medical Journal*, 2009**, 50**(3), 399-406.

41 D. R. Ciocca and S. K. Calderwood, *Cell Stress & Chaperones*, 2005**, 10**(2), 86-103.

42 E. Tiligada, *Endocrine-Related Cancer*, 2006**, 13**, S115-S124.

43 C. Dekker, P. C. Stirling, E. A. McCormack, H. Filmore, A. Paul, R. L. Brost, M. Costanzo, C. Boone, M. R. Leroux, and K. R. Willison, *Embo Journal*, 2008**, 27**(13), 1827-1839.

44 A. Castagna, P. Antonioli, H. Astner, M. Hamdan, S. C. Righetti, P. Perego, F. Zunino, and P. G. Righetti, *Proteomics*, 2004**, 4**(10), 3246-3267.

45 L. Yang, H. Y. Li, Y. Z. Jiang, J. Zuo, and W. Liu, *Cancer Letters*, 2013**, 336**(1), 213-221.

46 T. H. Davies and E. R. Sanchez, *Int. J. Biochem. Cell Biol.*, 2005**, 37**(1), 42-47.

47 W. S. Yang, H. G. Moon, H. S. Kim, E. J. Choi, M. H. Yu, D. Y. Noh, and C. Lee, *J. Proteome Res.*, 2012**, 11**(2), 1078-1088.

48 D. E. Epner and D. S. Coffey, *Prostate*, 1996**, 28**(6), 372-378.

49 B. Altenberg and K. O. Greulich, *Genomics*, 2004**, 84**(6), 1014-1020.

50 Y. Zhao, E. B. Butler, and M. Tan, *Cell Death. Dis.*, 2013**, 4**, e532.

51 S. Mori-Iwamoto, Y. Kuramitsu, S. Ryozawa, K. Mikuria, M. Fujimoto, S. I. Maehara, Y. Maehara, K. Okita, K. Nakamura, and I. Sakaida, *Int. J. Oncol.*, 2007**, 31**(6), 1345-1350.

52 F. Gong, X. Peng, Z. Zeng, M. Yu, Y. Zhao, A. Tong, *Mol Cell Biochem*., 2011, **348**(1-2), 141‑147.

53 X.D. Yan, L.Y. Pan, Y. Yuan, J.H. Lang, N. Mao, *J Proteome Res*., 2007, **6**(2), 772-780.

54 C.V. Dang, *BMC Biology,* 2013, **11**:3.

55 J.R. Doherty and J.L. Cleveland, *The Journal of Clinical Investigation*, 2013, **123**(9), 3685-3692.

56 M.L. McCleland ML, A.S. Adler, Y. Shang, T. Hunsaker, T. Truong, D. Peterson, E. Torres, L. Li, B. Haley, J.P. Stephan, M. Belvin, G. Hatzivassiliou, E.M. Blackwood, L. Corson, M. Evangelista, J. Zha J, R. Firestein, *Cancer Res*., 2012, **72**(22), 5812-5823.

57 Y. M. Go, J. R. Roede, D. I. Walker, D. M. Duong, N. T. Seyfried, M. Orr, Y. L. Liang, K. D. Pennell, and D. P. Jones, *Mol. Cell. Proteomics*, 2013**, 12**(11), 3285-3296.

58 P. Skehan, R. Storeng, D. Scudiero, A. Monks, J. Mcmahon, D. Vistica, J. T. Warren, H. Bokesch, S. Kenney, and M. R. Boyd, *J. Natl. Cancer Inst.*, 1990**, 82**(13), 1107-1112.

59 P. A. Modesti, T. Gamberi, C. Bazzini, M. Borro, S. M. Romano, G. E. Cambi, A. Corvi, W. Dorigo, L. Paparella, C. Pratesi, M. Carini, G. Gensini, and A. Modesti, *Anesthesiology*, 2009**, 111**(4), 844-854.

60 D. F. Hochstrasser, M. G. Harrington, A. C. Hochstrasser, M. J. Miller, and C. R. Merril, *Anal. Biochem.*, 1988**, 173**(2), 424-435.

61 N. A. Karp, M. Spencer, H. Lindsay, K. O'Dell, and K. S. Lilley, *J. Proteome Res.*, 2005**, 4**(5), 1867-1871.

62 S. M. N. Hunt, M. R. Thomas, L. T. Sebastian, S. K. Pedersen, R. L. Harcourt, A. J. Sloane, and M. R. Wilkins, *J. Proteome Res.*, 2005**, 4**(3), 809-819.

Figure Legends

Fig. 1 - Chemical structure of Aubipy$_c$.

Fig. 2 - Representative colloidal Coomassie blue silver-stained 2-DE gel images for A2780/R control cells (A) and Aubipy$_c$-treated A2780/R cells (**B**). Whole-cellular proteins (700 µg) were separated by 2-DE using IPG strips with a pH gradient of 3–10 nonlinear and 9–16% linear gradient SDS-PAGE. Protein spots were visualised by colloidal Coomassie blue silver staining. Black circles and numbers indicate statistically differentially abundant protein spots. Numbers correspond to spot number present in Table 2.

Fig. 3 - Functional classification of differentially abundant protein spots. The identified protein spots were sorted into functional categories based on the Gene Ontology (GO) terms related to their major biological functions using UniprotKB database (http://www.uniprot.org). In the histogram is reported the percentage of the identified proteins allocated in each functional category.

Fig. 4 - Functional GO Biological Process (BP) terms enrichment. GO BP terms statistically over-represented by 57 differentially abundant protein spots were achieved using the web-accessible program Database Annotation Visualization and Integrated Discovery v 6.7 (DAVID, http://david.abcc.ncifcrf.gov/home.jsp). The values in brackets are the *p*-values after Benjamini correction of each BP term. Detailed composition and statistical parameters of these GO terms were reported in Table S2.

Fig. 5 - Validation by Western blot of GAPDH and ENOA identity. Protein extracts (150 µg) from control and Aubipy$_c$-treated A2780/R cells were separated by 2-DE and transferred on a PVDF membrane. The blots were probed with antibodies against GAPDH and ENO1 proteins. The intensity of immune-stained spots was normalized with the corresponding protein spot intensity measured from the same blot stained with Coomassie brilliant blue. (**A**) Representative western blot images together with the 2-DE gel selected regions in which GAPDH and ENO1 localize and a representative Coomassie-stained PVDF membrane. Histograms visualize normalized mean relative-integrated-density ± standard deviation values of GAPDH (**B**) and ENO1 (**C**) spots (black bars: control cells; white bars: Aubipy$_c$-treated cells). For each protein, three independent experiments were carried out. The significance of abundance changes was performed by the two-tailed non-paired Student's-*t*-test using Graphpad Prism 6. The amount of each protein spot was statistically different between control and treated cells ($p<0.05$).

Fig. 6 - Metabolic investigations. A2780/R cells were treated for 48 h with $Aubipy_c$ concentration corresponding to its 72-h-exposure IC50 dose (10 µM). Glucose and Lactate amount was assessed in one millilitre of medium supernatant after 6, 12, 24 and 48 h of treatment. For each time point, three biological replicates were performed. The two-tailed non-paired Student's-*t*-test was carried out using Graphpad Prism 6. (**A**) Histogram reports the mean value ± SD of the glucose amount in culture medium expressed as µmoles of glucose/mg protein content. (**B**) Histogram reports the mean value ± SD of the lactate amount in culture medium expressed as µmoles of lactate/mg protein content. (**C**) For each time point, a western blot against LDHB was carried out. Representative immunoblots are shown together with representative Coomassie-stained PVDF membranes. Histogramm reports normalized mean relative-integrated-density ± SD values of LDHB band. For each time point, three independent experiments were carried out. The significance of abundance changes was performed by the two-tailed non-paired Student's-*t*-test using Graphpad Prism 6. (black bars: control cells; white bars: $Aubipy_c$-treated cells). A p-value<0.05 was considered statistically significant (*).

Table 1 Antiproliferative activity of Aubipy$_c$ and cisplatin against the A2780/R human ovarian carcinoma cell line, resistant to cisplatin

	A2780/R IC_{50} (μM) ± ES	
	24 h	**72 h**
Aubipy$_c$	28.87 ± 2.15	9.90 ± 0.10
n	3	3
Cisplatin	>100	24.89 ± 0.83
n	3	3

n, number of experiments; ES, standard error

Table 2 Differentially abundant protein spots identified by MALDI TOF mass spectrometry analysis

Spot No[†]	Protein name	AC[‡]	Gene Name	Cellular component Go term	Theoretical Mr (kDa)/ pI	Observed Mr (kDa)/ pI [§]	Mascot search results Score[¶]	Matched Pept.[‖]	Seq. coverage (%)[*]	Fold of variation (Aubipy$_c$ *vs* Control) [#]	ANOVA *p*-value[£]	*FDR* [⊥]
Stress response and Chaperones												
1	Heat shock 70 kDa protein 4L	O95757	HSPA4L	cytoplasm	95.5/5.6	97.0/5.7	262	32/57	41	-1.7	2.3E-04	9.9E-03
11	Heat shock 70 kDa protein 4L	O95757	HSPA4L	cytoplasm	95.5/5.6	70.1/5.4	281	31/52	46	1.2	1.2E-03	3.9E-02
18	T-complex protein 1 subunit beta	P78371	CCT2	cytoplasm	57.8/6.0	54.3/6.0	129	11/27	35	1.7	1.2E-04	6.8E-03
19	T-complex protein 1 subunit beta	P78371	CCT2	cytoplasm	57.8/6.0	54.0/6.1	144	15/59	46	1.5	1.3E-04	6.7E-03
6	Stress-70 protein, mitochondrial	P38646	HSPA9	mitochondrion	74.0/5.9	74.0/5.3	326	34/53	52	-4	3.1E-04	1.2E-02
7	Stress-70 protein, mitochondrial	P38646	HSPA9	mitochondrion	74.0/5.9	74.0/5.4	104	10/24	22	-2.3	5.0E-05	5.3E-03
16	Peptidyl-prolyl cis-trans isomerase FKBP4	Q02790	FKBP4	cytoplasm	52.0/5.3	55.9/5.3	131	14/51	40	-1.7	3.0E-05	4.9E-03
40	Activator of 90 kDa heat shock protein ATPase homolog 1	O95433	AHSA1	cytoplasm/ endo. reticulum	38.4/5.4	43.0/5.2	84	9/45	34	-1.4	2.9E-04	1.2E-02
Metabolism												
(Glucose Metabolism)												
31	Alpha-enolase	P06733	ENO1	cytoplasm	47.5/7.0	49.9/6.5	241	20/32	60	1.9	9.6E-06	2.5E-03
32	Alpha-enolase	P06733	ENO1	cytoplasm	47.5/7.0	49.4/7.2	205	17/50	52	1.6	1.3E-04	6.5E-03
48	Glyceraldehyde-3-phosphate dehydrogenase	P04406	GAPDH	cytoplasm	36.2/8.6	41.6/8.3	71	7/30	23	-2.6	1.0E-05	2.3E-03
52	Glyceraldehyde-3-phosphate dehydrogenase	P04406	GAPDH	cytoplasm	36.2/8.6	35.4/7.4	172	20/51	51	1.6	8.0E-05	6.9E-03
54	Glyceraldehyde-3-phosphate dehydrogenase	P04406	GAPDH	cytoplasm	36.2/8.6	36.7/7.9	88	12/51	42	1.3	3.0E-05	3.9E-03
37	Fructose-bisphosphatealdolase	P09972	ALDOC	cytoplasm	39.8/6.4	46.2/6.9	150	17/61	52	-4.0	9.0E-06	2.7E-03
49	L-lactate dehydrogenase B chain	P07195	LDHB	cytoplasm	36.9/5.7	36.7/5.5	212	25/52	61	-2.3	3.5E-04	1.3E-02
23	UTP--glucose-1-phosphate uridylyltransferase	Q16851	UGP2	cytoplasm/ endo. reticulum	57.1/8.2	53.6/7.8	86	10/43	27	1.4	2.4E-04	1.0E-02
(Cellular Respiration and ATP metabolism)												
25	ATP synthase subunit beta, mitochondrial	P06576	ATP5B	mitochondrion	56.5/5.3	51.8/5.2	78	9/49	29	-1.8	7.6E-06	3.4E-03
12	Dihydrolipoyl dehydrogenase, mitochondrial	P09622	DLD	mitochondrion	54.7/7.9	60.8/7.0	137	14/27	34	-3.9	9.0E-05	7.0E-03
39	Stomatin-like protein 2, mitochondrial	Q9UJZ1	STOML2	mitochondrion	38.6/6.9	43.7/5.2	133	11/35	47	-1.3	4.2E-04	1.4E-02
(Lipid Metabolism)												
35	Fatty acid synthase (fragment)	Q96IT0	FASN	cytoplasm/ mitochondrion	27.6/6.0	46.9/6.1	78	8/10	4	1.5	1.0E-04	6.9E-03
(Ketone Metabolism)												
20	Succinyl-CoA:3-ketoacid coenzyme A transferase 1,mitochondrial	P55809	OXCT1	mitochondrion	56.6/7.1	55.8/6.1	130	8/14	31	1.5	3.7E-04	1.3E-02
(Retinol Metabolism)												
15	Retinal dehydrogenase 1	P00352	ALDH1A1	cytoplasm	55.4/6.3	58.0/6.1	166	14/22	31	-3.4	1.7E-04	7.7E-03

				(Amino-acid and Protein Metabolism)								
13	Cytosol aminopeptidase	P28838	LAP3	cytoplasm	56.5/8.0	57.2/6.4	312	28/42	56	-4.4	1.0E-04	6.7E-03
14	Cytosol aminopeptidase	P28838	LAP3	cytoplasm	56.5/8.0	57.5/6.2	81	12/48	24	-2.7	4.0E-05	4.8E-03
47	3-hydroxyisobutyryl-CoA hydrolase, mitochondrial	Q6NVY1	HIBCH	mitochondrion	43.8/8.4	41.9/7.1	223	22/37	49	-4.2	2.9E-07	1.7E-04
46	Methionine adenosyltransferase 2 subunit beta	Q9H3E1	MAT2B	cytoplasm	37.9/6.9	40.9/7.5	192	13/29	46	1.4	1.5E-03	4.7E-02
55	S-methyl-5'-thioadenosine phosphorylase	Q9H010	MTAP	cytoplasm/ nucleus	31.7/6.7	31.4/7.0	103	8/30	54	-1.2	1.2E-04	6.5E-03
				(Purine Metabolism)								
9	Bifunctional purine biosynthesis protein PURH	P31939	ATIC	cytoplasm/ mitochondrion	65.1/6.3	66.5/6.3	350	31/50	39	-3.3	3.3E-04	1.2E-02
				Transport								
4	Mitochondrial inner membrane protein	Q16891	IMMT	mitochondrion	84.0/6.1	86.3/5.7	118	10/15	16	-3.5	1.0E-04	6.4E-03
5	Mitochondrial inner membrane protein	Q16891	IMMT	mitochondrion	84.0/6.1	84.1/5.9	109	9/16	15	-3.4	7.0E-05	6.3E-03
50	Transitional endoplasmic reticulum ATPase (fragment?)	P55072	VCP	endo. reticulum/ cytoplasm	89.9/5.1	35.6/5.0	74	9/38	15	3	2.0E-05	4.0E-03
				Protein synthesis								
2	Splicing factor, proline- and glutamine-rich	P23246	SFPQ	cytoplasm/ nucleus	76.2/9.4	95.0/9.2	114	13/31	25	1.9	1.4E-03	4.3E-02
8	Heterogeneousnuclearribonucleoprotein Q	O60506	SYNCRIP	nucleus	69.8/8.7	66.8/7.4	208	22/45	41	2.2	3.3E-04	1.2E-02
21	Elongation factor 2	P13639	EEF2	cytoplasm	96.2/6.4	52.2/6.9	159	19/64	25	1.5	6.0E-05	6.0E-03
33	Eukaryotic translation initiation factor 3 subunit G	O75821	EIF3G	cytosol/ nucleus	35.8/5.9	46.2/5.7	90	11/42	37	2.5	1.1E-04	6.4E-03
53	Heterogeneous nuclear ribonucleoproteins A2/B1	P22626	HNRNPA2B1	nucleus	37.4/8.9	37.3/7.9	62	9/53	22	1.4	6.0E-05	5.7E-03
57	Eukaryotic translation initiation factor 4H	Q15056	EIF4H	cytoplasm	27.4/6. 7	28.2/8.6	126	9/21	46	-1.6	3.3E-04	1.2E-02
41	Eukaryotic translation initiation factor 3 subunit I	Q13347	EIF3I	cytoplasm	36.9/5.4	42.4/5.3	117	9/23	32	-4	8.0E-05	6.6E-03
27	Zinc finger protein 18	P17022	ZNF18	nucleus	63.2/5.6	50.0/5.2	66	8/57	20	-1.4	1.0E-04	6.2E-03
42	THO complex subunit 3	Q96J01	THOC3	nucleus	39.4/5.7	42.0/5.6	128	16/58	39	1.2	2.4E-02	3.1E-02
45	Sialic acid synthase	Q9NR45	NANS	cytoplasm	40.7/6.3	42.0/6.6	103	13/65	40	-1.8	2.4E-04	9.8E-03
24	Plasminogen activator inhibitor 1 RNA-binding protein	Q8NC51	SERBP1	cytoplasm/ nucleus	45.0/8.7	55.6/8.7	118	10/18	24	1.4	9.0E-05	6.6E-03
				Cytoskeleton and Cell Structure								
3	Gelsolin	P06396	GSN	cytoskeleton	86.0/5.9	83.1/5.6	175	18/31	29	-1.6	9.0E-05	6.5E-03
26 (mix)#	Actin-like protein 6A Actin, cytoplasmic 1	O96019 Q96HG5	ACTL6A ACTB	cytoskeleton	47.9/5.4 42.0/5.3	49.6/5.2	105 73	12/59 7/59	39 30	-2.4	1.3E-04	6.3E-03
34	Actin, cytoplasmic 1 Actin, cytoplasmic 2	Q96HG5 P63261	ACTB ACTG1	cytoskeleton	42.0/5.3 42.1/5.3	45.9/5.2	116	11/44	42	-1.6	4.0E-05	4.5E-03
				Cell redox homeostasis								
17	Protein disulfide-isomerase A3	P30101	PDIA3	endo. reticulum	57.1/5.9	55.3/5.5	198	16/35	40	1.4	8.1E-08	1.5E-04
28	Glutathione synthetase	P48637	GSS	cytoplasm	52.5/5.7	50.9/5.4	159	16/50	40	1.2	1.9E-04	8.3E-03
				Cell cycle and apoptosis								

30	Proliferation-associated protein 2G4	Q9UQ80	PA2G4	cytoplasm/ nucleus	44.1/6.1	52.0/6.1	96	10/32	27	-3.3	3.2E-04	1.2E-02
38	Mitotic checkpoint protein BUB3	O43684	BUB3	cytoplasm/ nucleus	37.6/6.4	43.4/6.8	128	11/32	37	-1.8	2.0E-05	3.6E-03
22	26S protease regulatory subunit 8	P62195	PSMC5	cytoplasm	45.8/7.1	51.2/7.4	127	10/21	33	-4.6	1.2E-04	6.4E-03
56	Proteasome subunit alpha type-2	P25787	PSMA2	cytoplasm	26.0/6.9	29.8/7.1	122	9/28	56	-6.4	1.5E-04	7.1E-03
				Signal Transduction								
10	Ras GTPase-activating protein-binding protein 1	Q13283	G3BP1	membrane	52.2/5.4	64.7/5.3	211	19/60	59	-2.5	3.0E-05	4.5E-03
44	Annexin A1	P04083	ANXA1	membrane	38.9/6.6	40.3/6.3	98	13/51	42	-3.4	3.6E-04	1.3E-02
51	Annexin A1	P04083	ANXA1	membrane	38.9/6.6	37.6/6.1	201	12/14	42	1.8	8.0E-06	2.9E-03
43	PDZ domain-containing protein GIPC1	O14908	GIPC1	Cytoplasm/ membrane	36.1/5.9	41.8/6.0	192	18/33	55	-1.6	1.5E-04	6.9E-03
				DNA replication and repair								
29	RuvB-like 2	Q9Y230	RUVBL2	nucleus	51.3/5.5	52.1/5.3	178	18/52	45	-3.3	3.0E-05	4.2E-03
				Unknown								
36	WD repeat-containingprotein WRAP73	Q9P2S5	WRAP73		52.6/6.4	46.2/6.9	57	6/33	14	-3.5	1.4E-07	1.3E-04

† Spot numbers match those reported in the representative 2-DE images shown in Figure 2 (panel A and B).
‡ Accession number in Swiss-Prot/UniprotKB (www.uniprot.org/).
§ Based on the calculation using Progenesis SameSpots v4.0 software (Nonlinear Dynamics, UK).
¶ MASCOT MS score (Matrix Science, London, UK; http://www.matrixscience.com). MS matching score greater than 56 was required for a significant MS hit (*p*-value<0.05).
‖ Number of matched peptides corresponds to peptide masses matching the top hit from Ms-Fit PMF, searched peptide are also reported.
* Sequence coverage = (number of the identified residues/total number of amino acid residues in the protein sequence) x100%.
# Fold change (Aubipy$_c$-treated cells *vs* control cells) was calculated dividing the average of %V$_{Aubipy_c}$ by the average of %V$_{control}$. (V =volume=integration of the optical density over the spot area; %V = V single spot/V total spots included in the reference gel) using Progenesis SameSpots v4.0 software.
£ ANOVA test was performed by Progenesis SameSpots v4.0 software to determine if the relative change was statistically significant (p<0.05).
⊥ The False Discovery Rate (FDR) was calculated, using Excel 2013, in order to establish how many of the significant ANOVA *p*-values were false positives. Only the protein spots with an adjusted *p*-value (FDR)<0.05 were considered for the mass spectrometry analysis.

Table 3 Functional GO pathway enrichment analysis

Category	Pathway	Count[†]	Involved Genes	*p*-value[‡]	Benjamini[§]
KEGG_PATHWAY	Glycolysis / Gluconeogenesis (hsa00010)	5	Enolase1, alpha (P06733); Glyceraldehyde-3-phosphate dehydrogenase (P04406); Fructose-bisphosphatealdolase C (P09972); L-lactatedehydrogenase B (P07195); Dihydrolipoyldehydrogenase (P09622)	1,8E-04	8,3E-03
REACTOME_PATHWAY	Metabolism of carbohydrates (REACT_474)	6	Fructose-bisphosphatealdolase C (P09972); Enolase1, alpha (P06733); Glyceraldehyde-3-phosphate dehydrogenase (P04406); L-lactatedehydrogenase B (P07195); Dihydrolipoyldehydrogenase (P09622); UTP-glucose -1-phosphate uridylyltransferase (Q16851)	4,1E-04	9,7E-03

[†]Count indicates the number of the proteins /genes of our list involved in an enriched GO term.
[‡]*p*-value with a modified Fisher exact test was used to select the top enriched categories
[§]Benjamini multiple testing was performed to globally correct the *p*-value controlling family-wide false discovery rate (p-value ≤ 0.1).

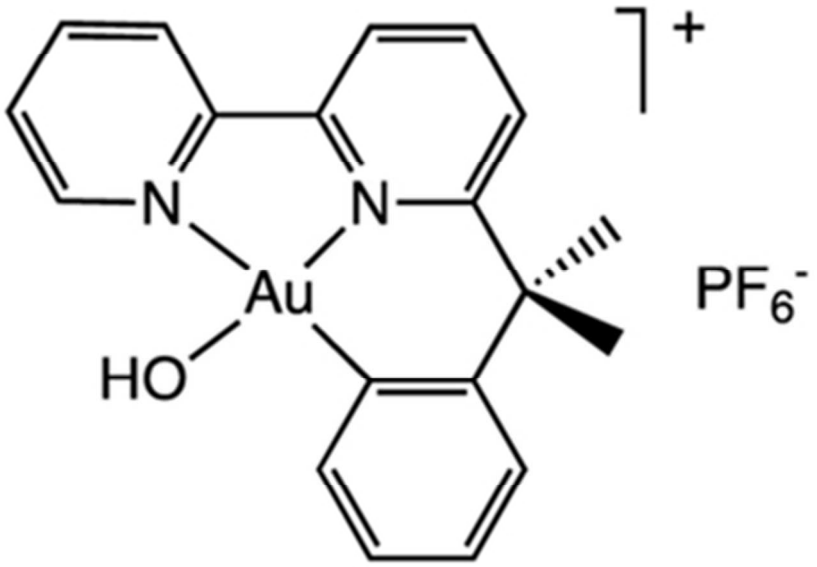

Chemical structure of Aubipyc.
36x27mm (300 x 300 DPI)

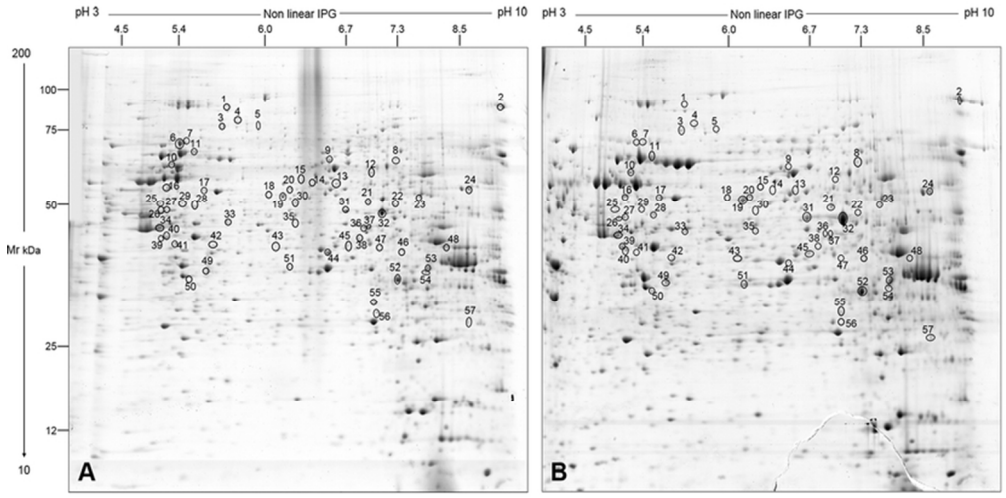

Representative colloidal Coomassie blue silver-stained 2-DE gel images for A2780/R control cells (A) and Aubipyc-treated A2780/R cells (B). Whole-cellular proteins (700 µg) were separated by 2-DE using IPG strips with a pH gradient of 3–10 nonlinear and 9−16% linear gradient SDS-PAGE. Protein spots were visualised by colloidal Coomassie blue silver staining. Black circles and numbers indicate statistically differentially abundant protein spots. Numbers correspond to spot number present in Table 2.
70x35mm (300 x 300 DPI)

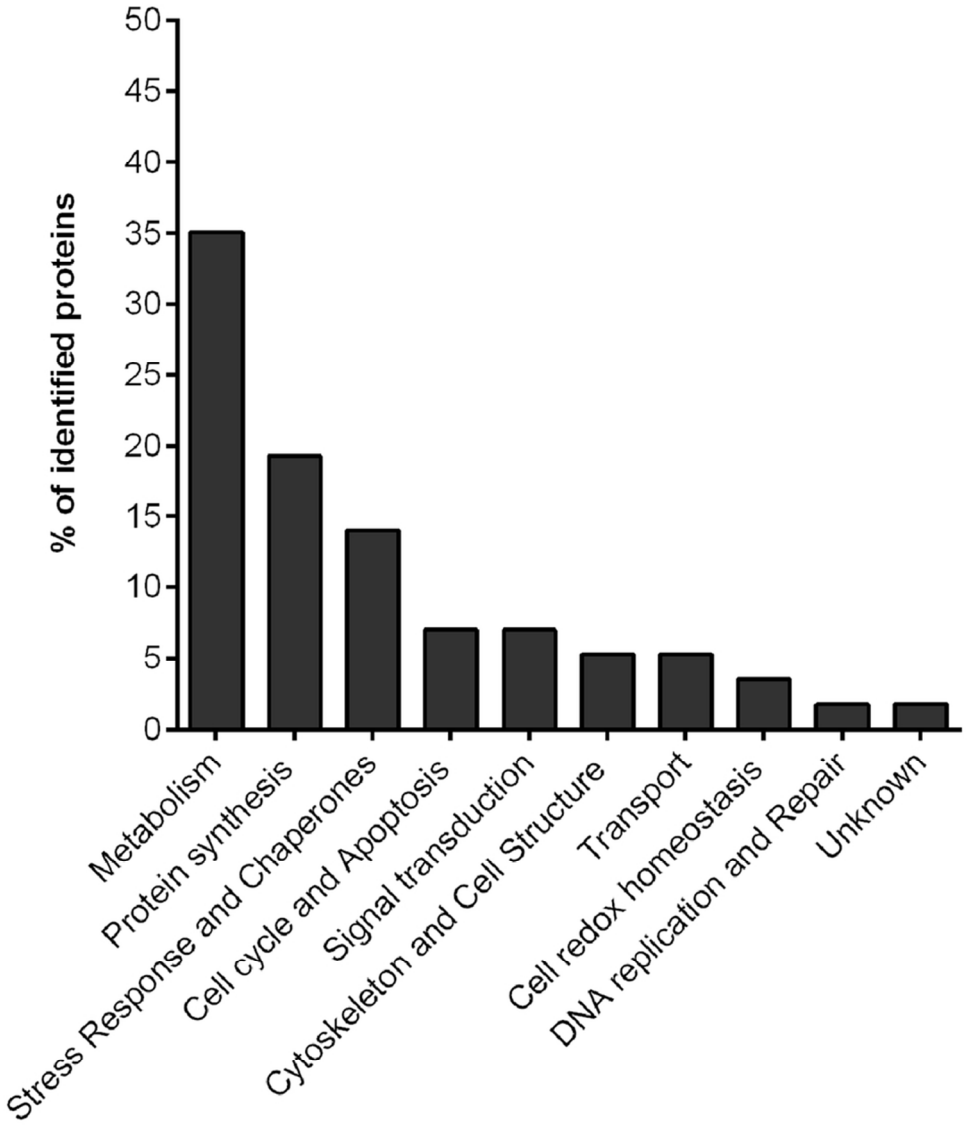

Functional classification of differentially abundant protein spots. The identified protein spots were sorted into functional categories based on the Gene Ontology (GO) terms related to their major biological functions using UniprotKB database (http://www.uniprot.org). In the histogram is reported the percentage of the identified proteins allocated in each functional category.
83x99mm (300 x 300 DPI)

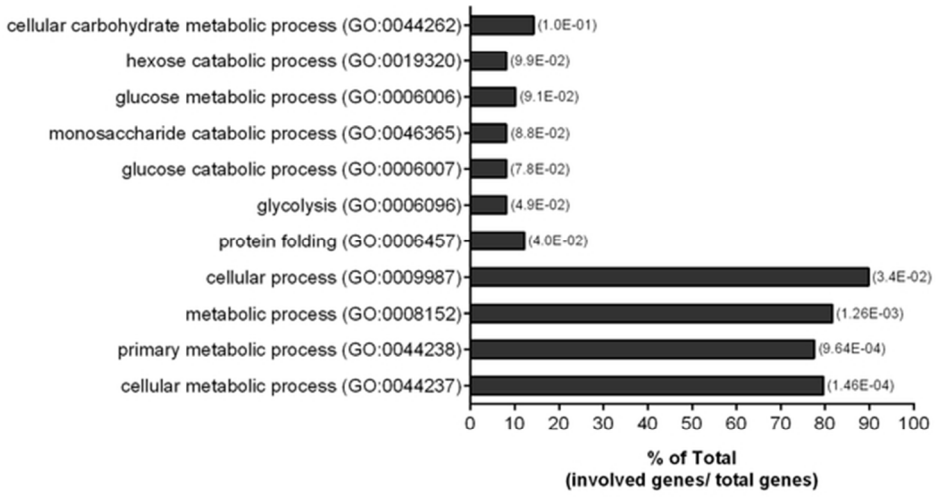

Functional GO Biological Process (BP) terms enrichment. GO BP terms statistically over-represented by 57 differentially abundant protein spots were achieved using the web-accessible program Database Annotation Visualization and Integrated Discovery v 6.7 (DAVID, http://david.abcc.ncifcrf.gov/home.jsp). The values in brackets are the p-values after Benjamini correction of each BP term. Detailed composition and statistical parameters of these GO terms were reported in Table S2.
56x31mm (300 x 300 DPI)

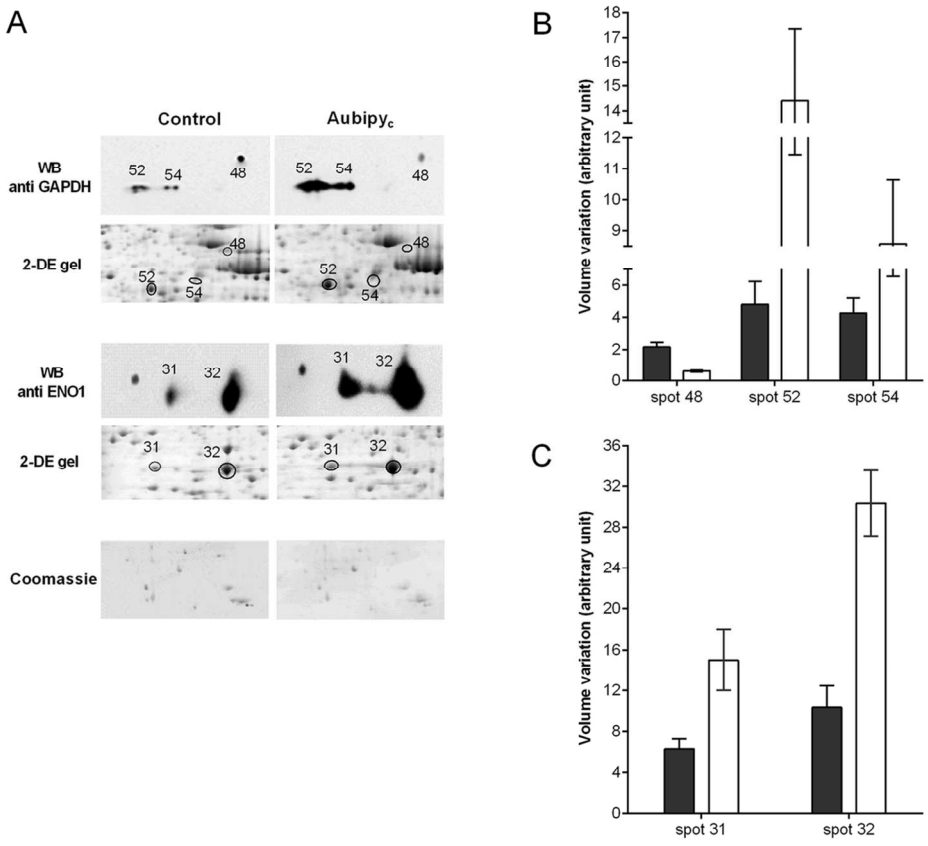

Validation by Western blot of GAPDH and ENOA identity. Protein extracts (150 µg) from control and Aubipyc-treated A2780/R cells were separated by 2-DE and transferred on a PVDF membrane. The blots were probed with antibodies against GAPDH and ENO1 proteins. The intensity of immune-stained spots was normalized with the corresponding protein spot intensity measured from the same blot stained with Coomassie brilliant blue. (A) Representative western blot images together with the 2-DE gel selected regions in which GAPDH and ENO1 localize and a representative Coomassie-stained PVDF membrane. Histograms visualize normalized mean relative-integrated-density ± standard deviation values of GAPDH (B) and ENO1 (C) spots (black bars: control cells; white bars: Aubipyc-treated cells). For each protein, three independent experiments were carried out. The significance of abundance changes was performed by the two-tailed non-paired Student's-t-test using Graphpad Prism 6. The amount of each protein spot was statistically different between control and treated cells ($p<0.05$).
107x97mm (300 x 300 DPI)

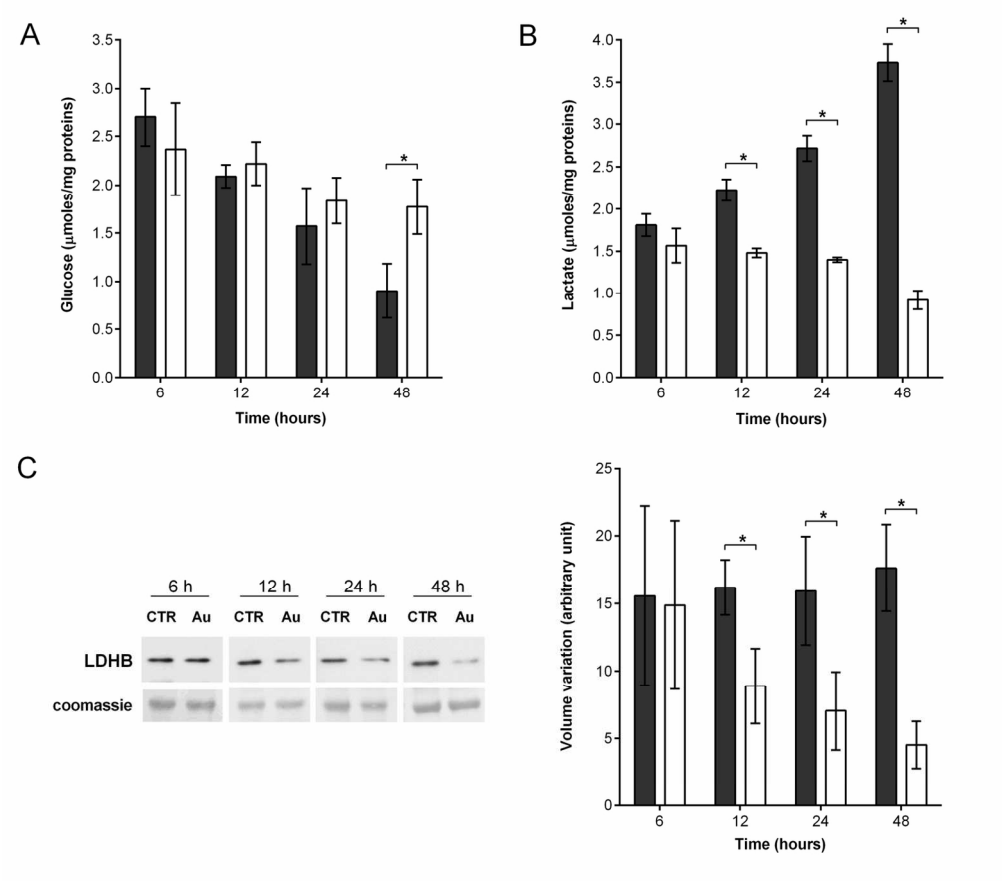

Metabolic investigations. A2780/R cells were treated for 48 h with Aubipyc concentration corresponding to its 72-h-exposure IC50 dose (10 µM). Glucose and Lactate amount was assessed in one millilitre of medium supernatant after 6, 12, 24 and 48 h of treatment. For each time point, three biological replicates were performed. The two-tailed non-paired Student's-t-test was carried out using Graphpad Prism 6. (A) Histogram reports the mean value ± SD of the glucose amount in culture medium expressed as µmoles of glucose/mg protein content. (B) Histogram reports the mean value ± SD of the lactate amount in culture medium expressed as µmoles of lactate/mg protein content. (C) For each time point, a western blot against LDHB was carried out. Representative immunoblots are shown together with representative Coomassie-stained PVDF membranes. Histogramm reports normalized mean relative-integrated-density±SD values of LDHB band. For each time point, three independent experiments were carried out. The significance of abundance changes was performed by the two-tailed non-paired Student's-t-test using Graphpad Prism 6. (black bars: control cells; white bars: Aubipyc-treated cells). A p-value<0.05 was considered statistically significant (*).
141x124mm (300 x 300 DPI)